

MODELLING DAILY EVAPOTRANSPIRATION USING ARTIFICIAL NEURAL NETWORKS UNDER HYPER ARID CONDITIONS

Mohamed A Yassin^{1,*}, A A Alazba^{1,2} and Mohamed A. Mattar^{2,3}

¹Alamoudi Water Chair, King Saud University, P.O. Box 2460, Riyadh 11451, Saudi Arabia; ²Agricultural Engineering Department, College of Food and Agriculture Sciences, King Saud University, P.O. Box 2460, Riyadh 11451, Saudi Arabia; ³Agricultural Engineering Research Institute (AEnRI), P.O. Box 256, Giza, Egypt.
*Corresponding author's e-mail: myassin1@ksu.edu.sa

Precisely determined evapotranspiration (ET) is necessary for maximization of water beneficiary use and hydrologic applications, particularly in arid and semiarid regions where water source is so limited, such as Saudi Arabia. Evapotranspiration is a complex, nonlinear process. However, data driven techniques can be used model it without requiring a complete understanding of the physics involved. Therefore, the Artificial Neural Networks (ANN) technique was used to estimate the daily reference evapotranspiration (ET_{ref}). Eight combinations of eight climatic parameters and crop height were used as input. The daily climatic variables were collected by 13 meteorological stations from 1980 to 2010. The ANN models were trained on 65% of the climatic data and tested using the remaining 35%. The generalised Penman-Monteith (PMG) model was used as a reference target for evapotranspiration values, with h_c varies from 5 to 105 cm with increment of a centimeter. The developed models were spatially validated using climatic data from 1980 to 2010 taken from another six meteorological stations. The results showed that the eight ET_{ref} models developed using the ANN technique to estimate ET_{ref} varies in significance depending on the climatic variables included. The more input climatic parameters included, the more accurate the ANN model is. The statistical performance criteria values such as determination coefficients (R^2) ranged from as low as 67.6% for ANN-MOD1, where air temperature is the only climatic parameter included, to as high as 99.8% for ANN-MOD8 with which all climatic parameters included. Furthermore, an interesting founded result is that the solar radiation has almost no effect on ET_{ref} under the hyper arid conditions. In contrast, the wind speed and plant height have a great positive impact in increasing the accuracy of calculating the daily reference evapotranspiration.

Keywords: Reference evapotranspiration, artificial neural network, Penman-Monteith model, alfalfa, grass, hyper arid.

INTRODUCTION

Water is the most important resource on the surface of the earth. Wherever water exists, life can be found. It is our duty to preserve, maintain and conserve this important resource. The water allocation to irrigated agriculture has recently decreased in arid and semi-arid regions where water is scarce. The Kingdom of Saudi Arabia (KSA) has limited water resources. Its geographical and astronomical features result in a warm, dry climate with little rainfall. Under the circumstances described, improvements to agricultural irrigation management and scheduling can greatly contribute to water conservation and the maintenance of sufficient levels of crop productivity and quality. Irrigation scheduling aims to replenish crop water requirements as quantified in evapotranspiration (ET) amounts (Ali, 2010). ET can be divided into the sub-processes evaporation and transpiration. Water passes into the atmosphere by evaporation from soil surfaces and by transpiration from plants (Allen *et al.*, 1998; Fangmeier *et al.*, 2006). ET can be determined either experimentally (directly) or mathematically (indirectly). It can be measured directly by using either a lysimeter or a water

balance in a controlled crop area (Gavilan *et al.*, 2007). However, this approach is difficult, time-consuming and expensive. Evapotranspiration can be calculated indirectly using a crop coefficient (K_c) as determined by the crop type, stage of growth, canopy cover and density and soil moisture, multiplied by a reference evapotranspiration (ET_{ref}) value (Allen *et al.*, 1998).

An accurate estimate of the ET_{ref} is crucial for studies on the hydrologic water balance, irrigation system design and management, crop production, water resources planning and management and environmental assessment (Irmak *et al.*, 2003; Temesgen *et al.*, 2005; Chattopadhyay *et al.*, 2009; Kumar *et al.*, 2011). The ET_{ref} is affected by the daily temperature, relative humidity, wind velocity, sunshine hours, atmospheric pressure, amount of matter dissolved in the water and the latitude. The ET_{ref} can be calculated by several methods that use climatological data and empirical relationships based on temperature, radiation, mass transfer or a combination which based on physical processes.

Monteith (1965) introduced a surface conductance term to account for the response of leaf stomata to their hydrological environment. This modified form of the Penman equation is

widely known as the General Penman-Monteith (PMG) evapotranspiration model (Monteith, 1973). This model is used by the United Nations' FAO (PMFAO) (Allen *et al.*, 1998) and ASCE-70 (Jensen *et al.*, 1990; Walter *et al.*, 2001; ASCE, 2005) as the most accurate method for calculating the ET_{ref} and to validate other equations. It incorporates thermodynamic and aerodynamic aspects, can be applied to a wide range of climatic contexts (Smith *et al.*, 1991; Yin *et al.*, 2008) and requires many climatic data inputs. This is especially true in developing countries, which have limited reliable climatic data sets of radiation, relative humidity and wind speed (Gocic and Trajkovic, 2010; Tabari and Talae, 2011).

Many studies have examined how other ET_{ref} equations with fewer data requirements perform against the PMG equation, to find alternative equations in the absence of some climatic data (e.g., George *et al.*, 2002; Xu and Singh, 2002; Fooladmand *et al.*, 2008; Sabziparvar and Tabari, 2010; Tabari, 2010). Temperature-based models, which are such as Hargreaves-Samani, Blaney-Cridde, and Thornthwaite, are some of the oldest methods for estimating the ET_{ref} (Xu and Singh, 2001). Radiation-based models, which are such as Priestley-Taylor, Jensen-Haise, Makkink, and Turc, have been widely used to estimate evapotranspiration from land areas (Xu and Singh, 2001), which is based on the energy balance (Jensen *et al.*, 1990). These models require calibration before extrapolating them to another environment (Kişi, 2006; Fooladmand and Haghighat, 2007).

Over the past decade, intelligent computational models have been developed as alternative methods for estimating the ET_{ref} , such as the artificial neural network (ANN) technique (Gorka *et al.*, 2008). ANNs are effective tools for modeling nonlinear processes, as they require few inputs and are able to map input-output relationships without any understanding of the physical process involved (Haykin, 1999; Sudheer *et al.*, 2003). Several studies have used ANN to estimate the ET_{ref} as a function of climatic variables. Kumar *et al.* (2002) indicated that their ANN model predicted the ET_{ref} better than the PMFAO method. Kumar *et al.* (2008) developed ANN models based on different categories of conventional ET_{ref} estimation methods, the temperature-based, radiation-based and combination models (PMFAO). All of the ANN models performed better than their respective conventional methods in estimating the PMFAO ET_{ref} . Landaras *et al.* (2008) compared seven ANN models with different input combinations with ten locally calibrated empirical and semi-empirical ET_{ref} models, using PMFAO daily ET_{ref} values as a reference. The results showed the ANN models obtained better results than the locally calibrated ET_{ref} equations. Huo *et al.* (2012) trained and tested ANN models to forecast the ET_{ref} using 50 years of climatic data from three stations in north-west China. They showed that the ANN models exhibited high precision compared to the other models. Our incomplete understanding of the physical

evapotranspiration process and a lack of the relevant data results in inaccurate ET_{ref} estimates. Simple, direct approaches with limited data requirements are needed. The objectives of this study are to: (1) Develop daily ET_{ref} models using the ANN technique from limited variables, (3) Spatially assess the developed daily ET_{ref} models, and (2) Assess the accuracy of the developed ANN models with PMFAO and PMASCE models.

MATERIALS AND METHODS

Study area and climatic data: The KSA is situated in the far southwest corner of Asia (Fig. 1), between latitudes $16^{\circ}22'46''N$ and $32^{\circ}14'00''N$ and longitudes $34^{\circ}29'30''E$ and $55^{\circ}40'00''E$. It is the largest country in Arabia. The KSA occupies about 70% of the area of the Arabian Peninsula with an approximate area of 1,950,000 km². It is divided into thirteen provinces, as shown in Figure 1. This study considers all of the provinces. The provinces are arranged by area in descending order in Table 1. The KSA's climate varies from region to region, depending on the terrain. The climate is generally characterized by hot summers, cold winters and winter rainfall. The central areas experience hot, dry summers and cool, dry winters. The coastal areas experience high humidity. The air temperature falls moderately with the onset of autumn, which lasts from 23 September to 21 December. The lowest air temperatures are reported in the northern regions ($3-7^{\circ}C$). Later in the year, temperatures significantly decline in other areas. Temperature variations are noted daily and vary from region to region.

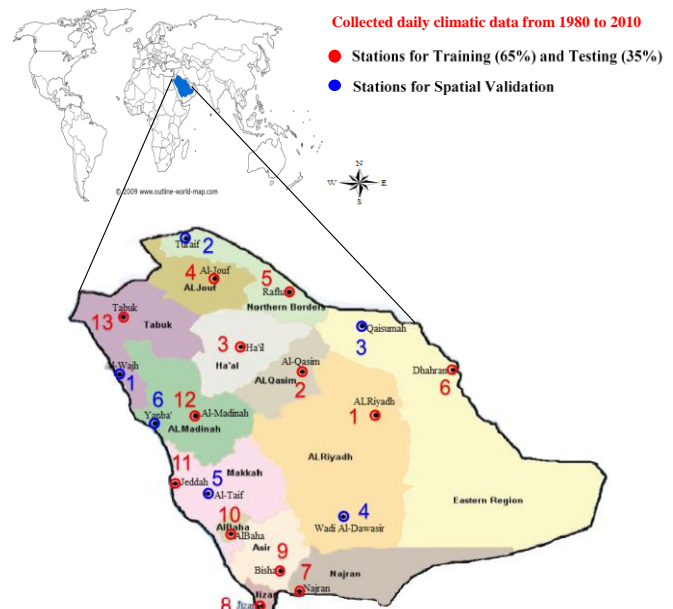


Figure 1. Map of the KSA, showing its provinces and meteorological stations.

Table 1. Meteorological station sites and climatic parameters.

Provinces	Areas* (km ²)	Stations	Location			Climatic Parameters							
			Longitude (deg)	Latitude (deg)	Altitude (m)	T _x (°C)	T _n (°C)	T _a (°C)	Rh _x (%)	Rh _n (%)	Rh _a (%)	U ₂ (m/s)	R _s (Mj/m ² /d)
Eastern region	540	Qaisumah	46.13	28.31	355	32	19	25	77	30	50	2.6	21
		Dhahran	50.20	26.30	17	33	20	26	75	29	52	4.2	20
Al-Riyadh	380	Riyadh (North)	46.72	24.93	614	33	20	26	38	16	31	3.9	15
		Wadi Al-Dawasir	45.20	20.50	617	35	22	28	35	17	26	3.4	18
Al-Madinah	150	Al-Madina	39.60	24.47	619	33	25	19	56	29	44	4.2	26
		Yanba'	38.10	24.10	1	29	22	17	78	23	50	3.2	29
Makkah	137	Jeddah	39.17	21.40	12	34	28	22	81	37	60	2.6	23
		Al-Ta'if	40.50	21.50	1449	35	29	23	60	29	39	3.2	27
Tabuk	136	Tabuk	36.58	28.38	770	29	14	22	53	17	32	2.9	33
		Al-Wajh	36.50	26.20	20	28	10	18	70	22	45	2.2	29
Najran	130	Najran	44.40	17.60	1214	35	29	25	60	33	44	3.5	28
Ha'il	120	Ha'il	41.70	27.40	1013	34	28	22	81	37	60	2.3	14
		Turaif	38.65	31.68	854	35	29	23	60	29	39	3.3	29
Northern borders	104	Rafha	43.50	29.60	447	29	14	22	53	17	32	2.9	22
		Al-Jouf	40.10	29.80	689	30	14	22	48	18	31	3.11	25
Asir	80	Bisha	42.60	20.00	1157	33	17	25	47	15	29	2.4	28
Al-Qasim	73	Al-Qasim	43.80	26.30	650	32	18	25	44	30	18	2.9	27
Jizan	13	Jizan	42.60	16.88	3	36	30	25	61	34	44	3.3	36
Al-Bahah	12	Al-Baha	41.60	20.30	1656	29	16	22	56	22	38	1.3	28

* Saudi Geological Survey (2012), King Saudi Arabia: Facts and Numbers, edition 1

For this study, climatic data was recorded at 19 meteorological stations selected from the 13 KAS provinces. The spatial distribution of the selected stations within the provinces is shown in Figure 1. Each province is represented by two stations, except for the provinces of Najran, Ha'il, Al-Jouf, Bisha, Al-Qasim, Jizan and Al-Baha, which are only represented by one station. The Presidency of Meteorology and Environment provided the data. The study's climatic data covers 31 years of daily meteorological information recorded from 1980 to 2010. The recorded data for all of the stations includes the maximum, minimum and mean air temperatures (T_x, T_n, and T_a) (°C); maximum, minimum and mean relative humidity (Rh_x, Rh_n and Rh_a) (%); wind speed at a 2m height (U₂) (m/s) and solar radiation (R_s) (Mj/m²/d). Table 1 describes the meteorological stations and lists the annual averages of the climatic data from each station.

The ANN models take at most nine input variables, T_x, T_n, T_a, Rh_x, Rh_n, Rh_a, U₂, R_s and the reference crop height (h_c) (m), which varies from 5 to 105 cm. This range is selected to cover both grass (10 to 15 cm) and alfalfa (30 to 80 cm). A random h_c value is chosen during training. The ET_{ref} is the output variable. The input variables are divided into three sets. The training set for the ANN models is composed of 65% of the daily data collected by 13 of the weather stations, Riyadh (North), Al-Qasim, Ha'il, Al-Jouf, Rafha, Dhahran, Najran, Jizan, Bisha, Al-Baha, Jeddah, Al-Madina and Tabuk, from 1980 to 2007. The training set is used to find the patterns present in the data. The testing set for the ANN models is composed of the remaining 35% of the data from the same weather stations and period as the training set. It is used to evaluate the generalization abilities of the trained models. The

ANN models' performances are checked once more with a validation data set. It is composed of the data collected by the remaining six weather stations, Turaif, Al-Wajh, Qaisumah, Yanba', Al-Ta'if and Wadi Al-Dawasir, from 1980 to 2010. The data is analyzed three times, using h_c = 5-105 cm, h_c = 12 cm and h_c = 50 cm.

Input parameters data of the ANN models: The ANN models take at most nine input variables, maximum, minimum and mean air temperature (T_x, T_n and T_a); maximum, minimum and mean relative humidity (Rh_x, Rh_n and Rh_a); wind speed (U₂); solar radiation (R_s) and the reference crop height (h_c), which varies from 5 to 105 cm. This range is selected to cover both grass (8 to 15 cm) and alfalfa (30 to 80cm). A random h_c value is chosen during training. The ET_{ref} is the output variable. The input variables are divided into three sets. The training set for the ANN models is composed of 65% of the daily data collected by 13 of the meteorological stations, Riyadh (North), Al-Qasim, Ha'il, Al-Jouf, Rafha, Dhahran, Najran, Jizan, Bisha, Al-Baha, Jeddah, Al-Madina and Tabuk, from 1980 to 2010. The training set is used to find the patterns present in the data. The testing set for the ANN models is composed of the remaining 35% of the data from the same meteorological stations and period as the training set. It is used to evaluate the generalization abilities of the trained models.

The ANN models' performances are checked once more with a validation data set. It is composed of the data collected by the remaining 6 meteorological stations, Turaif, Al-Wajh, Qaisumah, Yanba', Al-Ta'if and Wadi Al-Dawasir, from 1980 to 2010. The data is analysed three times, using hc= 5-105cm, hc= 12cm and hc=50cm.

Table 2. The input variables combinations used in the ANN technique.

Model	Input Parameters								
	Temperature(°C)			Relative Humidity (%)			u ₂ (m/s)	R _s (MJ/m ² /d)	h _c (m)
	T _x	T _n	T _a	Rh _x	Rh _n	Rh _a			
ANN-MOD1	✓	✓	✓						✓
ANN-MOD2	✓	✓	✓	✓	✓	✓			✓
ANN-MOD3	✓	✓	✓				✓		✓
ANN-MOD4	✓	✓	✓					✓	✓
ANN-MOD5	✓	✓	✓	✓	✓	✓	✓		✓
ANN-MOD6	✓	✓	✓	✓	✓	✓		✓	✓
ANN-MOD7	✓	✓	✓				✓	✓	✓
ANN-MOD8	✓	✓	✓	✓	✓	✓	✓	✓	✓

The input combinations: Several combinations of the input parameters were used as inputs to estimate the daily ET_{ref} using the ANN technique. The input parameter combinations are listed in Table 2. Eight ANN models were developed to test the performance of different combinations of input parameters, including climatic parameters and a reference h_c chosen randomly during the training process. The three temperature variables (T_x, T_n, and T_a) and h_c were included in all of the combinations.

The first combination used the three temperature elements and crop height. The second combination added the three humidity variables (Rh_x, Rh_n, and Rh_a) to the first combination. The third combination added U₂ to the first combination. The fourth combination added R_s to the first combination. The fifth combination was formed by inserting u₂ into the second combination. The sixth combination was formed by inserting R_s into the second combination. The seventh combination consisted of all inputs parameters except the relative humidity data. The eighth combination consisted of all the input parameters.

Output/targeted data of the ANN models: The performances of the ANN models are compared to the PMG method. The PMG method is considered the standard procedure when measured lysimeter data is not available (Irmak *et al.*, 2003; Gavilan *et al.*, 2006). The PMG method gives optimal results over all climatic zones (De Souza and Yoder, 1994; Chiew *et al.*, 1995; Hupet and Vanclooster, 2001; Naoum and Tsanis, 2003; Irmak *et al.*, 2003; Alazba, 2004; Gavilan *et al.*, 2006) and has advantages over many other mathematical equations. It can be used globally without any local calibrations due to its physical basis, is well-documented and has been validated with a significant amount of lysimeter data (Gocic and Trajkovic, 2010). Many researchers (Kumar *et al.*, 2002; Trajkovic, 2005; Kisi and Ozturk, 2007; Zanetti *et al.*, 2007; Landeras *et al.*, 2008; Jain *et al.*, 2008; Dai *et al.*, 2009; Traore *et al.*, 2010) have used the PMG equation as a reference and standard equation to evaluate the results of their mathematical models. The daily ET_{ref} values from the PMG equation are used as the output/target variables in the ANN and GEP models. A generalized form of the Penman-Monteith model can be written as (Alazba, 2004):

$$ET_{ref} = \lambda^{-1} \left[\frac{\Delta}{\Delta + \gamma^*} (R_n - G) + \frac{\gamma}{\Delta + \gamma^*} K (e_s - e_a) \right] \quad (1)$$

Where

- λ = latent heat of vaporization, (MJ.kg⁻¹);
- Δ = slope of the saturation vapour pressure-temperature curve at the mean air temperature (kPa.°C⁻¹);
- γ = psychrometric constant (kPa.°C⁻¹);
- R_n = net radiation (MJ.m⁻².day⁻¹);
- G = soil heat flux (MJ.m⁻².day⁻¹);
- γ* = modified psychrometric constant (kPa.°C⁻¹);
- K = parameter equal to $\frac{1.854 \times 10^5 \lambda / r_a}{T + 273}$ (MJ.m⁻².day. kPa)
- r_a = aerodynamic resistance (s.m⁻¹);
- T = air temperature (°C);
- e_s = saturation vapour pressure at the air temperature (kPa); and
- e_a = actual vapour pressure (kPa).

Description of artificial neural network ANN: ANN usually consists of layers of neurons, weights representing the connection strengths and a transfer or activation function. An ANN model of multilayer perception with a universal function approximator is used. Figure 2 depicts the model layers.

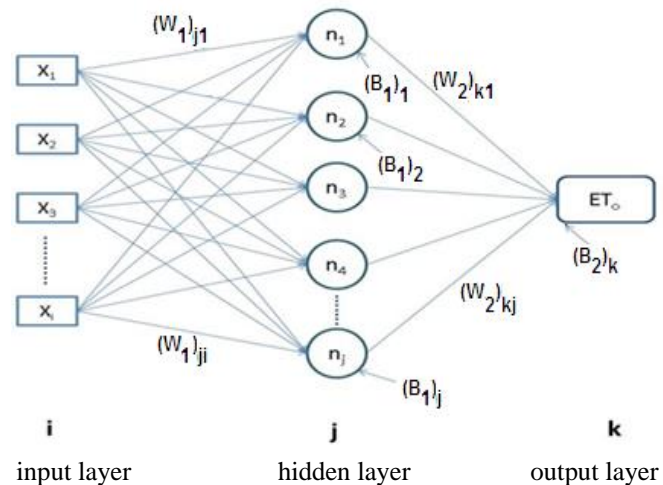


Figure 2. Architecture of the ANN used to model the ET_{ref}.

The input layer (i) is connected to the hidden layer (j), which is in turn connected to the output layer (k) by means of the connection weights (W) and biases (B). The W is used to change the throughput parameters and vary the connections to the neurons. The B is used as additional elements inside the hidden and output layer neurons. The neuron (processing element) in the hidden layer consists of aggregating weighted inputs, resulting in a quantity-weighted input (activation value). In the hidden layer, the neuron's activation value (h_j) is mathematically characterized using the following equation (Haykin 1999):

$$h_j = f\left(\sum_{i=1}^N (W_1)_{ji} X_i + (B_1)_j\right) \quad (2)$$

Where $(W_1)_{ji}$ is weights from the input layer to the hidden layer; X_i is input parameters; N is number of input neurons; $(B_1)_j$ is biases in the hidden layer; $f(\cdot)$ is activation (transfer) function.

Then, the output layer neuron (Y_k) is given by the following equation:

$$Y_k = f\left(\sum_{j=1}^n (W_2)_{kj} h_j + (B_2)_k\right) \quad (3)$$

Where $(W_2)_{kj}$ is weights from the hidden layer to the output layer; n is number of output neurons; $(B_2)_k$ is biases in the output layer.

The most common activation (transfer) functions in hydrological modeling are the sigmoid and hyperbolic tangent functions (Dawson & Wilby, 1998; Zanetti *et al.*, 2007). The hyperbolic tangent is similar to the sigmoid but can exhibit different learning dynamics during training. The sigmoid function is used in this study. Its general functional form is:

$$f(x) = \frac{1}{1 + \exp(-x)} \quad (4)$$

A feed-forward ANN that uses a back-propagation learning algorithm was employed in this study; as such ANNs are commonly used to estimate the ET_{ref} . The back-propagation learning algorithm optimizes the error function to modify the link weight. More than 70% of the existing studies that applied ANN techniques to hydrological processes used the back-propagation learning algorithm because of its simplicity and robustness (Kumar *et al.*, 2011). It controls the rate at which learning takes place using a momentum term and the learning rate. The momentum term is generally used to accelerate convergence and avoid local minima. A learning rate of 0.01 and a momentum factor of 0.8 are used.

Developing the ANN architecture: Software Multiple Back-Propagation version 2.2.4 was used to develop the ANN models to estimate the ET_{ref} . Nine input variables were used (the maximum input set of the ANN). The output as one neuron was in the output layer. The number of hidden neurons depended on several factors, such as the number of input and output neurons, the number of training cases, the amount of noise in the targets, the complexity of the function or

classification to be learned, the architecture, the type of hidden unit activation function and the training algorithm (Kumar *et al.*, 2011). The training data must be automatically normalized before they are exported to the ANN's feed-forward neural networks for training. Normalization is commonly between 0.15 and 0.85 in ANN modeling. The input data can flow after it is normalized. They undergo unidirectional processing from the input layer, through the hidden layer, to the output layer. In the hidden layer, each neuron receives input signals from the input layer through the weights (Izadifar, 2010). The data are processed separately by each hidden layer neuron and the outputs are passed to the output layer neuron.

The network output and target outputs are computed at the end of each forward pass in the forward-propagation stage. If an error is higher than a selected value, a reverse pass is performed to modify the connection weights by minimizing the error between the target and computed outputs (back-propagation stage). Otherwise, the training stops. The best number of hidden neurons in the hidden layer is found by training many ANNs and repeating the trial and error procedure (Jain *et al.*, 2008), taking into account the error values. The hidden layer initially has two nodes. The number of nodes increases in each trial by between one and four nodes, to a maximum of 20 nodes.

Performance criteria of ANN models: After training the ANN models, the ET_{ref} values were estimated and compared to the daily values from the PMG model. The comparisons were made using the following statistical parameters.

$$R^2 = \frac{\left(\sum_{i=1}^{n'} (E_i - \bar{E})(C_i - \bar{C})\right)^2}{\sum_{i=1}^{n'} (E_i - \bar{E})^2 \cdot \sum_{i=1}^{n'} (C_i - \bar{C})^2} \quad (5)$$

$$RMSE = \sqrt{\frac{\sum_{i=1}^{n'} (E_i - C_i)^2}{n'}} \quad (6)$$

$$OI = \frac{1}{2} \left(2 - \frac{RMSE}{E_x - E_n} + \frac{\sum_{i=1}^{n'} (E_i - C_i)^2}{\sum_{i=1}^{n'} (E_i - \bar{E})^2} \right) \quad (7)$$

$$MAE = \frac{\sum_{i=1}^{n'} |E_i - C_i|}{n'} \quad (8)$$

Where E_i is value of ET_{ref} estimated by the PMG; C_i is corresponding value calculated by mathematical ET_{ref} models; n' is number of observations; \bar{E} is average of the estimated values; \bar{C} is average of the calculated values; E_x is maximum estimated value; E_n is minimum estimated value.

RESULTS AND DISCUSSION

Choosing the ANN architecture: The optimal number of neurons in the hidden layers of an ANN must be determined through a trial and error procedure, as shown in Figure 2. Of

the eight ANNs tested, the simplified construct $N-2-1$ (where N is the number of neurons or input variables in the input layer) exhibits the poorest ANN performance, as reflected by the statistical indicators (Figs. 3 and 4). High values of R^2 and OI and low values of $RMSE$ and MAE , indicating good model

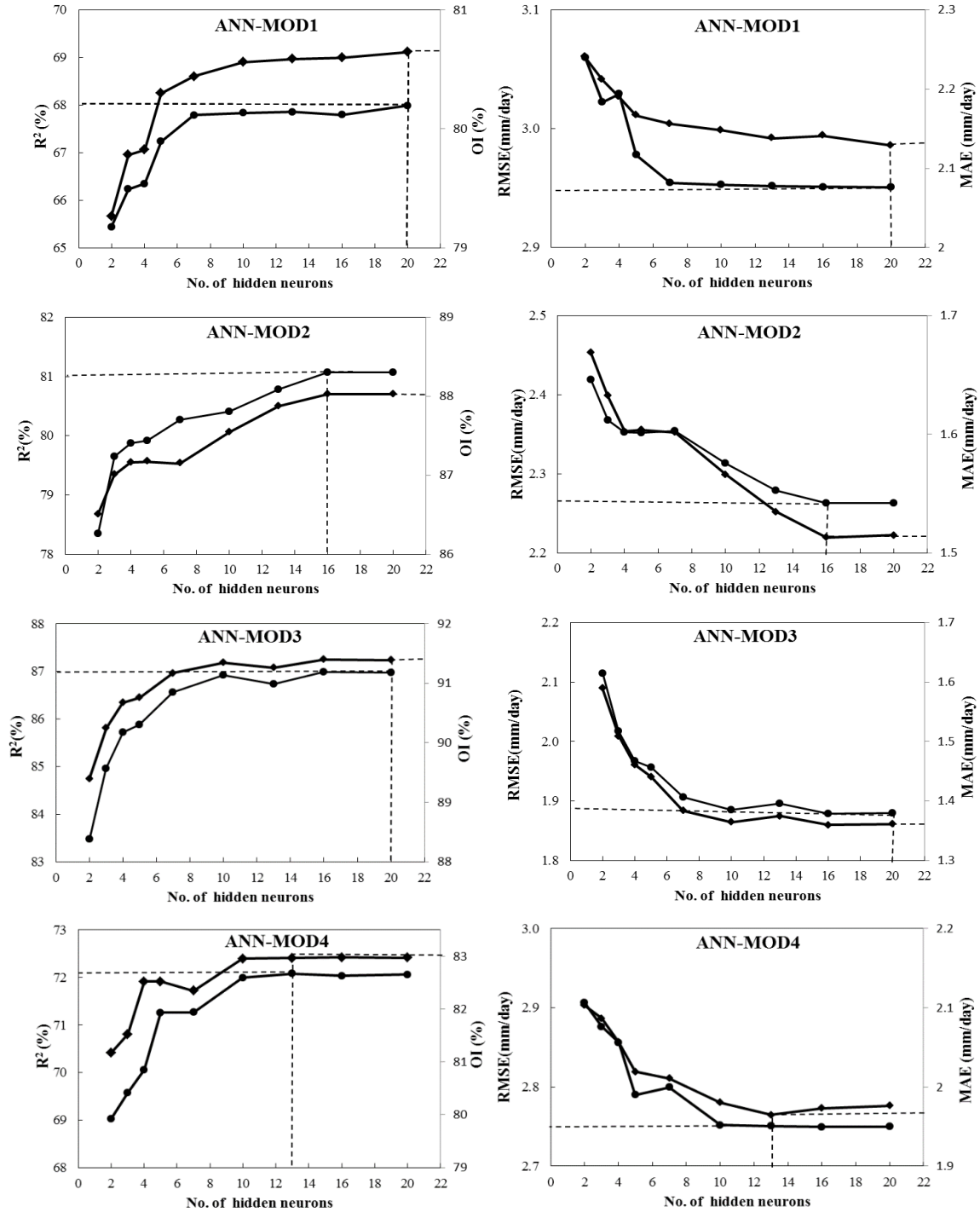


Figure 3. Accuracy of ANN-MOD1, ANN-MOD2, ANN-MOD3, and ANN-MOD4 in modelling the ET_{ref} using different numbers of hidden neurons during training, measured with R^2 , OI , $RMSE$ and MAE .

performance, are obtained by increasing n (where n is the number of neurons in the hidden layer) to more than two. It can be noted that a greater number of neurons in the hidden layer increases the structure complexity and does not improve the network behaviour. The optimum number of hidden layers represents the ET_{ref} nonlinear complex relationship (Kumar *et al.*, 2002; Zanetti *et al.*, 2007). The numbers of neurons in the

hidden layer of the ANN models used for the various training models were 2, 3, 4,....., 20. The networks were trained over up to 20,000 iterations, as there were negligible improvements (increases in the R^2 and decreases in the $RMSE$) after 20,000 iterations.

For example, ANN-MOD1 was trained using up to 20 processing elements. The optimum results are found using 20

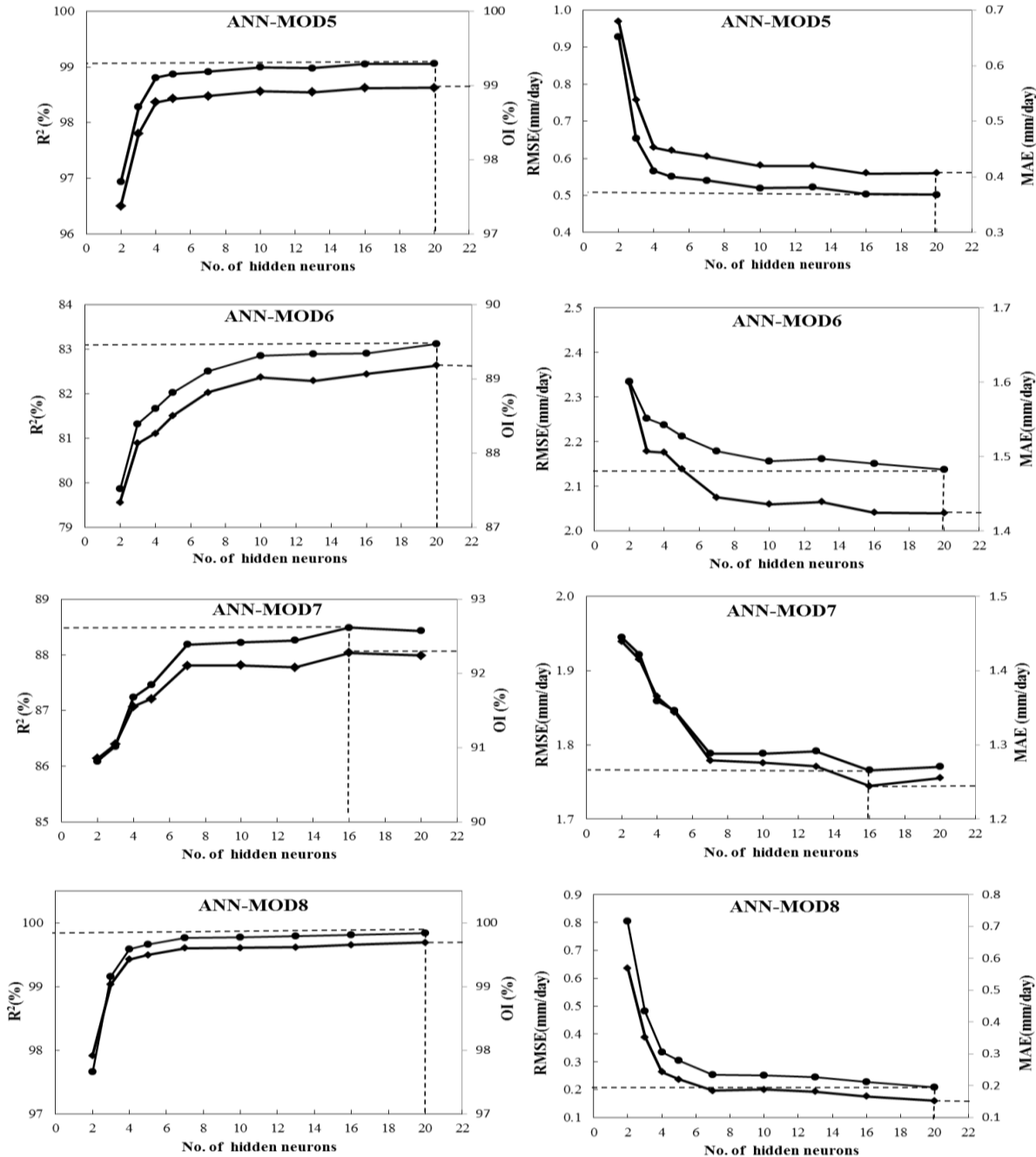


Figure 4. Accuracy of ANN-MOD5, ANN-MOD6, ANN-MOD7, and ANN-MOD8 in modeling the ET_{ref} using different numbers of hidden neurons during training, measured with R^2 , OI , $RMSE$ and MAE .

neurons, generating the maximum R^2 (68.0 %) and OI (80.7%) values and the minimum $RMSE$ (2.95 mm/d) and MAE (2.13 mm/d) values for the training set, as shown in Figure 3. The best ANN-MOD1 model for forecasting the daily ET_{ref} is composed of one input layer with four input variables, the daily maximum, mean, and minimum air temperature and the crop height, one hidden layer with 20 neurons and one output layer with one output variable. The rest of the ANN models were also tested to determine the optimum number of neurons in their hidden layers. The best ANN models for each input combination and their performance statistics on the training data set are shown in Figures 3 and 4.

The following steps were used to formulate the ANN models:

$$ET_{ref(ANN-MODk)} = \frac{(ET_{ref})_{nk} - 0.15}{(0.85 - 0.15)} \times (ET_{ref\ max} - ET_{ref\ min}) + ET_{ref\ min} \tag{9}$$

where $(ET_{ref})_{nk}$ is the normalized value and $ET_{ref(ANN-MODk)}$ is the actual value for the ET_{ref} in any model. The $ET_{ref\ max}$ is 45.72 mm/day and the $ET_{ref\ min}$ is 0.46 mm/day.

$$ET_{ref(ANN-MODk)} = \frac{(ET_{ref})_{nk} - 0.15}{(0.85 - 0.15)} \times (45.72 - 0.46) + 0.46 \tag{10}$$

Eq. 14 is further simplified to:

$$ET_{ref(ANN-MODk)} = 64.65(ET_{ref})_{nk} - 9.24 \tag{11}$$

$$(ET_{ref})_{nk} = \left(1 + \exp\left(-\sum_{j=1}^N W_{jk} F_j + B_k\right) \right)^{-1} \tag{12}$$

where the weights (W_{jk}) and the biases (B_k) are given in

Table A1. The parameter F_j is computed from:

$$F_j = \left(1 + \exp\left(-\sum_{i=1}^n w_{ij} x_i + b_j\right) \right)^{-1} \tag{13}$$

where the weights (w_{ij}) and the biases (b_j) are given in Tables A2-A9 and x_i is the input variable. The subscripts i, j and k represent the number of input, hidden and output neurons, respectively. The mathematical formulations are easily programmed in a spreadsheet (i.e. Microsoft Excel) or in the Visual Basic programming language to predict the ET_{ref} using Equations 9-13, along with Tables A1 and A2-A9.

Table A1. Biases and Weights for ANN models at the output layer.

Model , K	Bias B _k	Weights from the hidden layer to the output layer																			
		W _{k1}	W _{k2}	W _{k3}	W _{k4}	W _{k5}	W _{k6}	W _{k7}	W _{k8}	W _{k9}	W _{k10}	W _{k11}	W _{k12}	W _{k13}	W _{k14}	W _{k15}	W _{k16}	W _{k17}	W _{k18}	W _{k19}	W _{k20}
1	1.60	-1.95	0.77	-0.02	0.37	1.44	-0.96	-0.12	-0.95	-4.44	0.20	2.07	1.53	-0.87	1.98	-0.01	0.76	2.02	2.36	-0.07	-7.13
2	4.87	-0.48	0.12	-0.21	0.35	-10.96	0.31	-0.32	-0.52	-6.62	-0.63	-0.10	-0.33	-0.90	-0.66	0.68	-3.26	-	-	-	-
3	0.59	-0.29	1.24	-1.16	-1.77	-1.11	0.78	-0.66	1.51	-1.13	-2.74	-0.66	-0.12	-0.56	-1.00	-2.68	1.30	-	-	-	-
4	0.06	0.70	-0.16	-2.35	0.31	-4.90	-2.58	4.61	1.45	-1.39	0.16	-0.64	-0.73	-0.51	-	-	-	-	-	-	-
5	-0.11	0.26	-4.75	-0.63	-0.83	-0.65	-0.48	0.09	-2.30	-0.68	0.50	2.49	-0.70	-0.88	-1.58	-1.23	-0.31	-0.14	1.29	0.81	-0.90
6	0.78	-8.75	-0.64	-1.55	-3.03	1.16	3.15	-0.47	2.83	0.32	2.17	1.90	-6.84	2.10	1.66	0.37	0.52	1.69	-3.48	0.27	-0.69
7	0.35	-0.43	-1.08	-1.24	-0.58	-4.32	0.44	-0.74	0.44	3.02	-1.09	-2.50	0.81	-1.78	2.33	-2.97	0.88	-	-	-	-
8	0.77	7.27	-1.83	-0.39	-1.01	-0.48	-0.60	-5.70	-0.64	-2.29	1.54	-0.37	-10.96	-0.92	-0.72	0.76	-0.34	-1.71	1.02	0.41	-0.86

Table A2. Biases and Weights for ANN-MOD1.

No. of hidden neuron, j	bias (b _j)	Weights from the input layer to the hidden layer			
		W _{j1}	W _{j2}	W _{j3}	W _{j4}
1	-1.967	9.021	-0.438	4.496	0.087
2	-6.203	-0.198	0.977	0.188	0.932
3	-0.322	-0.709	2.298	-0.104	-0.009
4	-0.700	-1.197	0.180	3.473	0.342
5	-1.443	-0.058	0.130	1.210	1.615
6	-0.559	-1.852	4.163	-0.428	4.257
7	2.706	-0.498	2.699	-0.409	-0.107
8	4.147	0.148	8.311	-0.590	0.933
9	-3.496	0.116	-0.469	0.524	-2.731
10	0.095	1.585	0.491	0.157	2.623
11	5.305	-0.423	0.247	0.566	0.211
12	1.750	0.306	0.854	-0.713	0.416
13	-1.992	5.337	-12.615	5.084	0.119
14	-1.339	0.020	0.608	-0.043	0.852
15	-1.714	0.003	1.735	0.100	0.762
16	-0.052	3.913	1.203	1.420	0.955
17	0.043	2.345	5.230	4.710	0.301
18	0.250	-4.001	2.533	0.615	1.075
19	1.961	-0.336	1.998	-0.348	0.148
20	5.628	-1.053	1.013	-0.751	-0.120

Table A3. Biases and Weights for ANN-MOD2.

No. of hidden neuron, j	bias (b _j)	Weights from the input layer to the hidden layer						
		w _{j1}	w _{j2}	w _{j3}	w _{j4}	w _{j5}	w _{j6}	w _{j7}
1	-8.628	2.955	5.786	1.159	2.147	-2.737	-0.852	0.405
2	-5.142	0.533	6.747	-2.948	-0.170	2.776	-10.320	1.744
3	-6.543	0.753	7.173	2.473	8.572	2.090	1.329	-0.758
4	-7.595	1.591	5.997	7.982	5.857	4.222	-2.187	0.135
5	-1.152	-0.028	-0.159	-0.488	0.066	-0.011	0.107	-0.148
6	-4.225	-0.890	4.904	1.961	-3.746	4.431	-1.934	0.284
7	-11.651	2.166	11.014	-5.425	-4.370	1.192	-10.048	-0.274
8	-16.890	16.192	5.106	-5.225	-0.271	-1.131	-2.424	1.968
9	-5.193	-0.324	1.448	-0.933	-0.088	-0.050	-0.408	-2.499
10	-7.185	15.265	-1.438	2.879	-4.531	8.553	0.996	0.419
11	11.237	-11.098	-12.585	-9.846	-12.125	1.294	-13.789	0.287
12	-5.550	4.283	4.924	3.156	-0.894	4.329	7.202	0.365
13	-3.454	0.067	-0.179	-0.506	3.865	1.801	-0.912	0.579
14	3.222	-1.194	-11.912	13.334	0.901	3.244	0.009	-0.155
15	-4.070	11.519	-1.951	-0.794	-2.194	4.208	0.534	0.278
16	6.846	-3.020	-3.736	1.332	1.243	0.027	-0.041	-1.252

Table A4. Biases and Weights for ANN-MOD3.

No. of hidden neuron, j	bias (b _j)	Weights from the input layer to the hidden layer				
		w _{ji}	w _{j2}	w _{j3}	w _{j4}	w _{j5}
1	-3.280	29.503	10.441	-37.704	0.967	0.262
2	1.583	1.501	-1.059	1.229	1.915	-0.634
3	-0.858	-8.260	12.099	-5.928	0.614	0.484
4	3.669	0.939	-2.374	-2.779	-2.658	-0.813
5	-0.305	-1.965	3.844	-5.192	2.304	-0.244
6	-0.830	-0.652	-0.434	0.958	0.905	2.295
7	-1.035	-4.925	-13.450	14.654	1.127	0.322
8	-0.898	0.596	-0.800	1.424	-1.310	0.638
9	-1.687	-1.350	0.638	0.726	-1.050	0.223
10	-4.001	0.027	-0.519	0.114	0.856	-3.464
11	-0.752	-1.603	0.780	0.385	0.054	-0.023
12	-0.444	-3.693	0.085	-1.394	2.125	0.642
13	-0.068	-0.562	-0.113	-0.723	-0.208	0.312
14	-1.014	-0.788	0.550	-0.208	-0.938	-0.093
15	-3.035	0.980	0.110	-0.457	-2.718	-0.124
16	-0.849	-3.939	12.736	-12.426	1.889	-0.089

Table A5. Biases and Weights for ANN-MOD4.

No. of hidden neuron, j	bias (b _j)	Weights from the input layer to the hidden layer				
		w _{ji}	w _{j2}	w _{j3}	w _{j4}	w _{j5}
1	-2.057	-1.846	0.778	0.950	-0.108	2.967
2	-8.766	-5.698	21.721	2.622	-1.565	1.678
3	-1.799	-3.122	0.668	0.634	-1.097	0.408
4	-1.006	-1.253	2.222	-1.074	1.454	3.587
5	-3.871	0.371	-0.274	-0.204	-0.284	-2.557
6	-1.223	-0.030	-1.915	-0.115	0.944	0.339
7	-8.255	-2.636	4.681	-1.770	5.936	0.451
8	-4.047	-2.072	3.937	5.138	-1.865	0.375
9	-3.578	-4.865	9.281	-2.484	0.068	0.680
10	11.504	6.039	-14.710	-14.474	-2.430	-0.062
11	1.072	4.420	-0.997	-0.401	-5.181	-0.033
12	2.889	-10.626	4.170	-3.928	1.292	0.461
13	-2.892	3.218	1.706	7.044	-0.372	-0.169

Table A6. Biases and Weights for ANN-MOD5.

No. of hidden neuron, j	bias (b _j)	Weights from the input layer to the hidden layer							
		W _{j1}	W _{j2}	W _{j3}	W _{j4}	W _{j5}	W _{j6}	W _{j7}	W _{j8}
1	-1.967	6.977	-0.332	2.074	-0.554	2.946	0.347	0.082	-0.065
2	-6.203	0.444	0.599	-1.098	-0.626	0.137	-0.059	-4.585	0.245
3	-0.322	-1.587	-0.008	0.075	0.657	-0.085	-0.462	-0.443	0.306
4	-0.700	-0.597	0.353	-0.428	0.564	1.242	-0.558	0.444	0.066
5	-1.443	-0.551	-0.410	0.264	-0.776	0.492	-0.500	0.503	-1.415
6	-0.559	-1.609	-0.884	2.820	-0.352	1.215	-0.367	0.420	-0.129
7	2.706	6.443	-2.903	3.604	-0.188	2.328	7.614	3.931	0.469
8	4.147	-2.855	-1.590	1.856	1.159	0.562	0.000	-2.617	-1.311
9	-3.496	-3.850	-1.301	-1.107	0.418	0.009	0.755	-0.136	-0.279
10	0.095	-1.374	-0.645	0.719	0.650	0.451	2.266	0.007	-0.134
11	5.305	-0.387	-0.113	0.680	0.297	0.119	-0.277	-0.993	5.807
12	1.750	-0.952	-1.248	-0.735	0.432	0.198	0.877	1.831	-0.054
13	-1.992	-0.891	-0.702	1.225	0.353	-0.414	-0.934	-0.788	-0.189
14	-1.339	0.971	-1.548	-0.197	1.700	0.737	-0.298	1.958	0.490
15	-1.714	1.391	0.415	-2.335	0.301	-0.299	1.522	-0.640	-0.394
16	-0.052	-4.411	-2.231	0.170	-0.201	0.222	0.884	-1.446	-0.229
17	0.043	-1.668	1.638	0.694	-1.079	1.470	0.578	0.197	-0.735
18	0.250	0.013	0.776	-1.331	-0.501	-0.442	-0.391	2.080	0.880
19	1.961	-0.359	-0.852	-0.607	-0.309	0.016	-0.809	1.836	0.242
20	5.628	0.045	0.167	0.312	0.274	0.010	-0.252	-1.047	7.787

Table A7. Biases and Weights for ANN-MOD6.

No. of hidden neuron, j	bias (b _j)	Weights from the input layer to the hidden layer							
		W _{j1}	W _{j2}	W _{j3}	W _{j4}	W _{j5}	W _{j6}	W _{j7}	W _{j8}
1	-4.521	0.504	1.616	-1.945	-0.181	-0.293	-0.088	0.058	-1.836
2	-4.231	3.227	5.027	-5.084	3.567	0.047	1.003	-0.308	0.415
3	-23.004	3.234	5.148	3.960	-1.325	-0.413	-3.751	8.852	1.194
4	-10.916	1.017	8.772	4.385	-5.703	5.515	2.598	-0.105	0.281
5	-9.806	-2.830	5.234	7.152	-0.539	1.491	-0.930	1.043	0.316
6	-12.175	3.544	12.067	-11.253	-5.974	-0.085	-0.196	1.139	1.157
7	-10.787	-0.007	4.443	1.237	-6.313	2.815	-8.010	-0.570	0.297
8	-15.188	-5.425	10.754	3.024	1.562	1.127	-4.302	3.193	1.603
9	-3.177	-11.991	-1.004	14.030	-0.293	-0.338	-1.751	-1.286	2.557
10	-4.109	4.714	-2.094	0.505	-2.083	1.590	1.404	-0.748	1.386
11	-12.182	-3.961	6.104	6.575	0.177	0.961	-1.691	1.717	0.872
12	-0.975	-0.153	-0.930	0.126	0.301	0.199	0.029	-0.277	-0.104
13	-9.110	-0.035	3.205	5.347	0.550	2.434	1.341	-0.943	-1.222
14	-12.911	2.982	7.076	-3.213	-3.648	-1.816	4.177	3.374	1.107
15	-3.717	11.371	21.022	-29.622	-1.075	-0.438	-1.332	0.606	0.421
16	-9.532	-5.748	4.206	5.290	-10.150	0.397	0.022	-0.408	-0.498
17	-10.297	-1.288	4.792	5.413	-0.938	1.546	-0.554	1.218	0.187
18	-5.218	0.791	-0.612	0.706	-0.476	-0.029	-1.289	-0.830	-0.152
19	-7.188	14.386	-14.106	5.796	2.538	-2.205	-2.629	-8.715	0.531
20	15.850	-1.972	-2.721	1.864	1.445	1.321	-0.397	-11.818	-0.871

Table A8. Biases and Weights for ANN-MOD7.

No. of hidden neuron, j	bias (b_j)	Weights from the input layer to the hidden layer					
		w_{j1}	w_{j2}	w_{j3}	w_{j4}	w_{j5}	w_{j6}
1	4.887	-2.879	4.062	-1.826	7.762	-0.037	-0.359
2	-0.531	-1.191	-6.410	3.966	1.640	-0.601	0.323
3	-3.696	0.823	-0.329	2.014	3.153	1.943	-1.195
4	-2.638	17.962	3.787	-17.283	2.877	-0.232	0.471
5	-2.500	0.151	-0.337	-0.156	-2.241	-0.239	-0.077
6	-4.915	-19.695	22.119	-10.330	-2.032	1.781	-0.008
7	0.801	-6.742	0.693	5.204	4.953	-0.130	-0.453
8	0.071	0.225	0.481	0.198	1.506	-0.932	1.364
9	-4.077	-1.204	3.695	2.641	1.449	-1.233	0.901
10	5.236	2.197	-4.159	-0.979	-2.776	-4.461	-0.100
11	-6.899	0.413	-0.266	-0.429	1.021	-0.461	-6.169
12	0.816	-0.118	-0.318	0.587	2.514	-0.121	0.482
13	-1.159	-3.847	4.591	-2.535	0.097	-0.358	0.107
14	-0.742	0.862	1.114	0.018	1.950	-0.099	0.410
15	-2.521	-2.534	4.128	0.442	0.549	-0.009	0.837
16	-0.547	0.451	-0.764	-0.594	-0.187	0.418	0.701

Table A9. Biases and Weights for ANN-MOD8.

No. of hidden neuron, j	bias (b_j)	Weights from the input layer to the hidden layer								
		w_{j1}	w_{j2}	w_{j3}	w_{j4}	w_{j5}	w_{j6}	w_{j7}	w_{j8}	w_{j9}
1	-5.361	2.163	1.185	-1.071	-1.072	-0.388	-0.083	1.978	0.229	1.037
2	-2.492	1.283	-1.196	-0.424	1.558	0.034	-0.241	0.111	-0.467	0.249
3	-0.805	0.426	-0.152	-1.311	0.871	0.297	0.670	-1.253	0.601	-0.556
4	-1.065	-0.662	-0.726	1.182	0.910	0.668	-0.216	-2.551	0.848	-0.723
5	-0.928	0.318	0.283	1.037	-0.402	0.120	0.449	-2.206	-0.925	-0.416
6	0.264	-1.054	-0.703	0.488	0.899	0.377	-0.519	-1.709	-0.544	0.881
7	-7.374	0.203	0.337	-0.571	-0.588	-0.273	0.154	-5.405	-0.465	0.206
8	-1.336	-0.949	-0.301	-0.869	-0.247	0.712	-0.513	0.048	-0.864	-0.230
9	-3.748	0.989	-0.913	-0.101	1.622	2.107	0.071	0.719	-0.362	0.294
10	-1.658	1.356	0.450	-1.637	-0.915	-0.513	0.126	1.220	-1.511	0.466
11	-0.488	0.214	-0.928	-0.594	0.246	0.143	0.330	0.024	-1.448	0.133
12	-9.374	0.111	0.039	-0.337	-0.024	-0.014	-0.026	0.524	-0.044	-7.406
13	10.179	-0.074	-0.001	0.251	-0.308	-0.154	0.324	0.195	-0.115	10.418
14	-0.676	0.516	-0.137	-0.540	-0.056	-0.007	-0.248	1.862	-0.195	-1.662
15	0.857	1.481	-0.755	0.036	0.931	0.509	0.289	2.129	0.554	0.204
16	-1.094	0.700	-0.557	-1.030	0.494	0.353	1.428	0.567	0.334	-0.730
17	-0.740	-0.657	-0.772	-0.178	0.311	0.018	0.124	1.827	-0.191	0.196
18	-1.937	1.308	0.983	-0.411	-0.805	-0.276	0.139	-1.887	0.333	0.331
19	-0.362	-0.995	-2.051	0.267	1.578	0.365	-0.302	-0.125	-0.342	-0.653
20	-3.082	0.235	0.474	0.293	-1.213	-0.762	0.147	-1.064	-0.522	-0.528

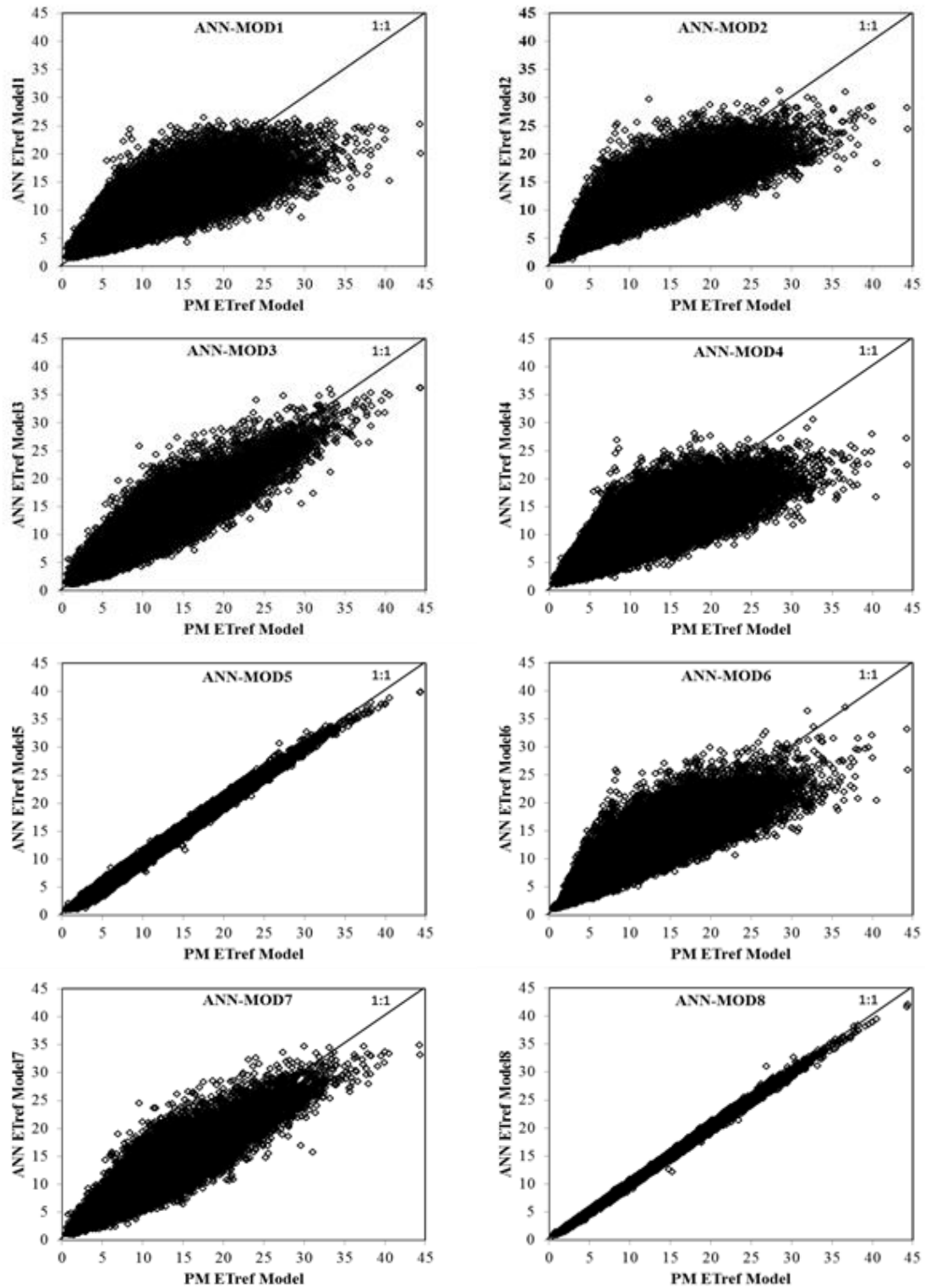


Figure 5. Comparison of the daily ET_{ref} estimated using the ANN models with different input combinations during training process and the PMG equation, using 65% of the data collected from 1980 to 2010 Jby 13 meteorological stations.

ANN Models Performance:

Training and testing processes: Figure 5 shows that the daily ET_{ref} values estimated by the ANN models that used U_2 during the training process matched well with each other and the values estimated by the PMG model. The effectiveness of these models is clear. The scatter plots for the training process in Figure 5 also show that the ANN-MOD5 and ANN-MOD8 data mostly follow the 45° line. However, many points in the ANN models that do not use U_2 are located above and below this line.

Table 3 presents the statistical results of the optimum ANN models using different input combinations to estimate the ET_{ref} . In training, it can be observed that the absence or presence of some of the input variables in the input sets significantly affects the models' performances. The ANN-MOD1 temperature-based model only took the three temperature variables. ANN-MOD1 performed worst, with R^2 of 67.9%, OI of 80.6%, $RMSE$ of 2.95 mm/d and MAE of 2.12 mm/d (Table 3). The ANN-MOD2 performed better than ANN-MOD1 that had a R^2 and OI values that were about 18% and 8.4% increase, due to the presence of the three humidity variables. While the ANN-MOD2 had an $RMSE$ and MAE values that were about 21.4% and 25%, respectively, more accurate than that from the ANN-MOD1. This is confirmed by the Figure 6 that shows an importance ratio analysis of each input parameter used in the calculation of the daily ET_{ref} . The figure shows that T_n of 37.66% and 22.31% were the most significant parameters affecting ANN-MOD1 and ANN-MOD2, respectively. As the average importance ratio of three humidity variables was 12.72% in ANN-MOD2.

Additionally, ANN-MOD3 predicative accuracy increased, whereas the R^2 was 87.1%, a 28.3% and 8.6% increase over the R^2 values of ANN-MOD1 and ANN-MOD2, respectively. The rest of statistical criteria for the ANN-MOD3 confirm that ET_{ref} performs poorly without U_2 . The importance ratio of U_2 and T_n were also the second most influential variables, both nearly 19%. Moreover ANN-MOD4, which added R_s to the ANN-MOD1 combination, improved slightly on estimating ET_{ref} than ANN-MOD2. This is evident in Figure 6 that T_n of 28.55% and T_x of 24.28% were the dominant input variables.

However, inserting U_2 into ANN-MOD2, as in ANN-MOD5,

resulted in a dramatic increase in R^2 from 80.2% to 99.1%, i.e. a 19.98% increase. The $RMSE$ and MAE values indicate that the ANN-MOD5 performs better than the ANN-MOD2, indicating a decrease of 78.4% and 74.7%, respectively. The value of OI is close to one which supports the argument that the ET_{ref} can perform well without R_s . The T_x of 20.32% and U_2 of 17% had also the largest effect on ANN-MOD5 (Fig. 6). As, switching ANN-MOD5's R_s for U_2 , as in ANN-MOD6, resulted in a intense decrease in the values of R^2 and OI that were 16.6% and 10.2% less accurate than that from the ANN-MOD5. The $RMSE$ and MAE for ANN-MOD6 were almost three times that of the values for the ANN-MOD5. This is in accordance with Kişi and Ozturk (2007).

Comparing ANN-MOD7's results with those of the other ANN models shows that the accuracy of the ANN-MOD4 was significantly improved by the inclusion of U_2 , as ANN-MOD7 had a 22.7% and 11.2% increase in the R^2 and OI over ANN-MOD4, receptivity. The $RMSE$ and MAE for ANN-MOD7 had also 36.1% and 37.2% % more accurate than that from the ANN-MOD4. U_2 (24.49%) was the most significant parameters affecting ANN-MOD7. This is in agreement with Hupet and Vanclooster (2001). U_2 is likely to be an effective, powerful variable for accurately modelling the nonlinear complex process of ET_{ref} (Fisher *et al.*, 2005; Xiaoying and Erda, 2005; Li and Beswick, 2005; Traore *et al.*, 2010). On the other hand, the statistical criteria in Table 3 indicate that slight difference between the ANN-MOD6 and the ANN-MOD2, also between the ANN-MOD7 and the ANN-MOD3. This shows that R_s had an insignificant influence (about of 8.5%) on estimating ET_{ref} . Finally, ANN-MOD8, which has the full input set similar to the PMG model, performs better than the rest of the ANN models, whereas the R^2 value indicated a strong fit to the data. The ANN-MOD8 yielded a highest OI and a lowest $RMSE$ and MAE .

In testing, Table 3 show the results of adding either the three humidity variables (ANN-MOD2), U_2 (ANN-MOD3) or R_s (ANN-MOD4) to ANN-MOD1. ANN-MOD2 and ANN-MOD3 performed better than ANN-MOD1. A slightly worse performance was obtained for ANN-MOD4. This result indicates that R_s had a slight effect on modelling the ET_{ref} , as the R^2 value increased by 6.65% only when R_s was added to ANN-MOD1.

Table 3. Statistical performance of the optimized ANN models during training and testing.

Model	Inputs	Training				Testing			
		R^2 (%)	OI (%)	$RMSE$ (mm/d)	MAE (mm/d)	R^2 (%)	OI (%)	$RMSE$ (mm/d)	MAE (mm/d)
ANN-MOD1	T_x, T_n, T_a, hc	67.9	0.806	2.95	2.12	67.6	0.803	3.00	2.20
ANN-MOD2	$T_x, T_n, T_a, Rh_x, Rh_n, Rh_a, hc$	80.2	0.874	2.32	1.59	80.4	0.875	2.33	1.61
ANN-MOD3	T_x, T_n, T_a, u_2, hc	87.1	0.914	1.87	1.35	87.1	0.914	1.89	1.33
ANN-MOD4	T_x, T_n, T_a, R_s, hc	72.2	0.830	2.74	1.96	72.1	0.827	2.78	2.04
ANN-MOD5	$T_x, T_n, T_a, Rh_x, Rh_n, Rh_a, u_2, hc$	99.1	0.989	0.50	0.40	99.1	0.989	0.51	0.41
ANN-MOD6	$T_x, T_n, T_a, Rh_x, Rh_n, Rh_a, R_s, hc$	82.6	0.888	2.17	1.45	82.3	0.885	2.22	1.53
ANN-MOD7	$T_x, T_n, T_a, u_2, R_s, hc$	88.6	0.923	1.75	1.23	88.8	0.924	1.76	1.19
ANN-MOD8	$T_x, T_n, T_a, Rh_x, Rh_n, Rh_a, u_2, R_s, hc$	99.8	0.996	0.21	0.15	99.8	0.997	0.19	0.14

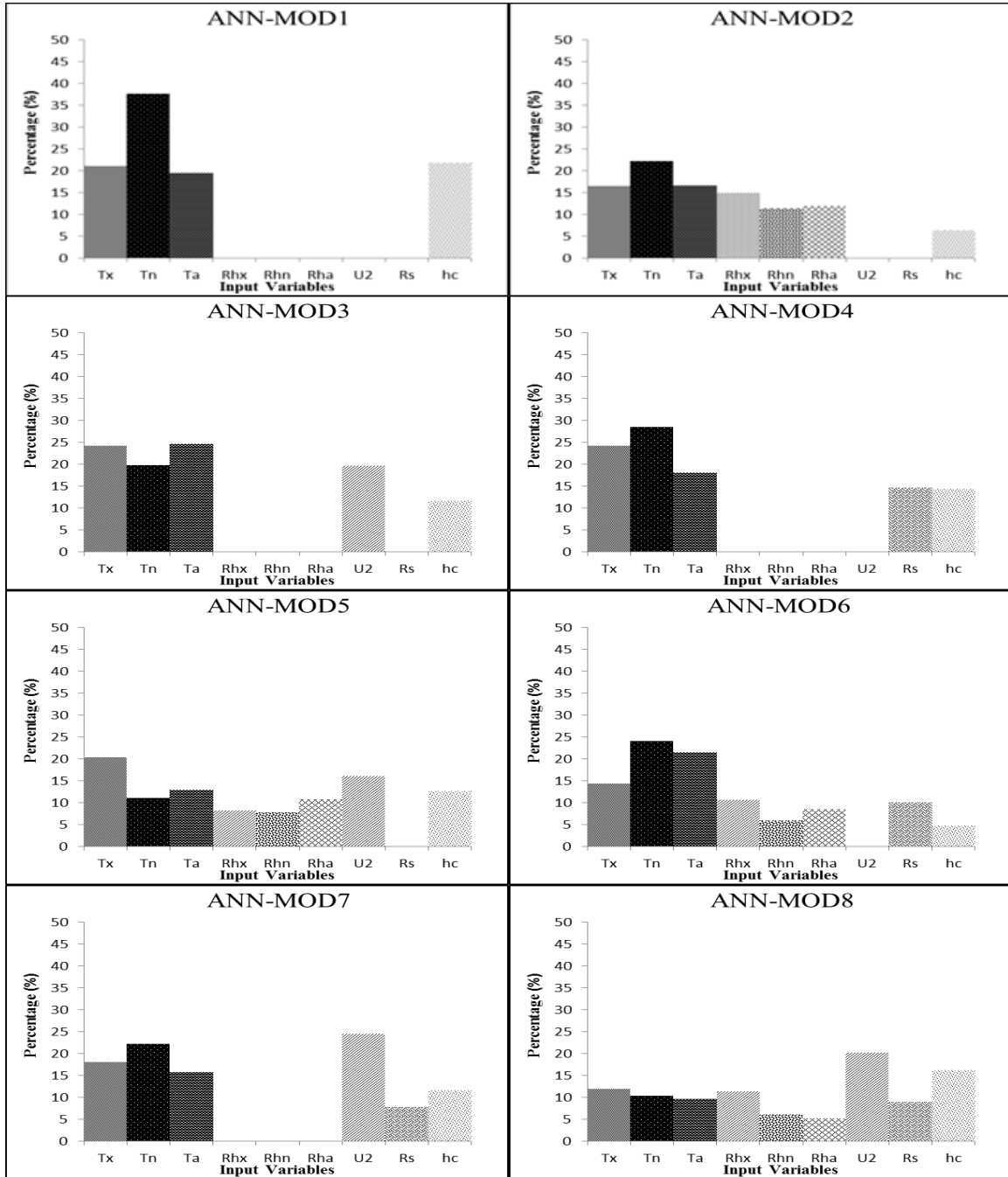


Figure 6. Importance ratio analysis of the input variables in the ANN models.

The relative humidity variables seemed to be more effective than R_s in the modelling of the ET_{ref} , as the R^2 increased by 18.93% when the humidity variables were added to ANN-MOD1. Adding U_2 to the input combination improved the estimation accuracy significantly, due to its advection effects on the ET_{ref} (Kishi, 2007), as the R^2 increased by 28.84% when U_2 was added to ANN-MOD1.

Similarly, U_2 and R_s were separately added to ANN-MOD2. The R^2 increased drastically from 80.4 to 99.1%, i.e., a 23.56% increase, when U_2 was added to ANN-MOD2. However, the inclusion of R_s in ANN-MOD2 did not significantly increase the R^2 value (a 2.36% increase results). Furthermore, R_s increased the R^2 slightly by 2.36% when it was added to ANN-MOD3. This result indicates that R_s had an insignificant effect on ET_{ref} modelling. The ANN-MOD8 model

Table 4. Statistical performance of the optimized ANN models during validation, using data collected from 1980 to 2010 by six meteorological stations.

Model	Inputs	h _c =105				h _c 50				h _c 12			
		R ² (%)	OI (%)	RMSE (mm/d)	MAE (mm/d)	R ² (%)	OI (%)	RMSE (mm/d)	MAE (mm/d)	R ² (%)	OI (%)	RMSE (mm/d)	MAE (mm/d)
ANN-MOD1	T _x ,T _n ,T _a ,h _c	66.6	79.2	3.19	2.23	61.2	76.1	2.87	2.12	68.4	76.2	1.84	1.32
ANN-MOD2	T _x ,T _n ,T _a ,Rh _x ,Rh _n ,Rh _a ,h _c	83.1	87.5	2.41	1.61	79.1	85.5	2.17	1.50	80.4	81.9	1.58	1.16
ANN-MOD3	T _x ,T _n ,T _a ,u ₂ ,h _c	83.9	89.2	2.22	1.59	82.8	87.4	2.01	1.50	85.1	89.3	1.17	0.88
ANN-MOD4	T _x ,T _n ,T _a ,R _s ,h _c	66.5	79.9	3.13	2.19	62.3	77.1	2.81	2.08	73.4	81.0	1.63	1.14
ANN-MOD5	T _x ,T _n ,T _a ,Rh _x ,Rh _n ,Rh _a ,u ₂ ,h _c	98.9	98.8	0.56	0.44	98.4	98.3	0.59	0.47	95.6	94.8	0.77	0.60
ANN-MOD6	T _x ,T _n ,T _a ,Rh _x ,Rh _n ,Rh _a ,R _s ,h _c	85.1	88.8	2.27	1.45	82.2	87.4	2.01	1.32	85.2	85.2	1.41	1.03
ANN-MOD7	T _x ,T _n ,T _a ,u ₂ ,R _s ,h _c	83.1	88.3	2.32	1.63	82.1	86.3	2.11	1.54	86.6	90.8	1.08	0.78
ANN-MOD8	T _x ,T _n ,T _a ,Rh _x ,Rh _n ,Rh _a ,u ₂ ,R _s ,h _c	99.8	99.7	0.21	0.15	99.8	99.3	0.29	0.22	99.4	98.2	0.38	0.30

outperformed all of the other models on all of the performance criteria.

Spatial assessment of ANN models: The effectiveness of the ANN models can be demonstrated by estimating the ET_{ref} at other sites, validating the reliability and stability of these models. As mentioned previously, the validation process used three crop height values. Using h_c=5-105 cm gave a maximum ET_{ref} value of 40 mm/day. The ANN models' R² values ranged from 66.6 to 99.8%, OI values from 79.2 to 99.7%, RMSE values from 0.21 to 3.19 mm/day and MAE values from 0.15 to 2.23 mm/day as shown in Table 4. Comparing the model performance criteria with h_c=5-105 cm showed little difference between the training and validation processes. The ratio of variation in the R² between the training and validation processes for ANN-MOD1 (1.95%), ANN-MOD5 (0.20%) and ANN-MOD8 (0.0%) indicated that these models have good network activity. In contrast, the ratio of variation in the R² increased slightly for ANN-MOD2 (3.48%), ANN-MOD3 (3.82%) and ANN-MOD6 (2.93%). The ratio increased drastically for ANN-MOD4 (8.57%) and ANN-MOD7 (6.61%).

The ANN models were tested using h_c = 50 cm to validate their feasibility on alfalfa and h_c=12 cm to validate their feasibility on grass. The maximum ET_{ref} was 35 mm/day on alfalfa and 25 mm/day on grass. The ANN models on alfalfa had R² values ranging from 61.2 to 99.8%, RMSE values from 0.29 to 2.87 mm/day, OI values from 76.1 to 99.3% and MAE values from 0.22 to 2.12 mm/day (Table 4). The ANN models on grass had R² values from 68.4 to 99.4%, RMSE values from 0.38 to 1.84 mm/day, OI values from 76.2 to 98.2% and MAE values from 0.30 to 1.32 mm/day.

The R² value decreased on alfalfa for ANN-MOD1 (11.76%), ANN-MOD2 (1.64%), ANN-MOD3 (2.77%), ANN-MOD4 (17.81%), ANN-MOD6 (3.64%) and ANN-MOD7 (5.48%), indicating that these models performed better on grass than on alfalfa (Table 4). However, the R² value decreased on grass for ANN-MOD5 (2.84%) and ANN-MOD8 (0.40%), indicating that these models performed slightly better on alfalfa than on grass.

ANN vs. PMFAO and PMASCE: In both cases grass and alfalfa, a comparison between the best models has been made

which is ANN-MOD8. The 1:1 line in Figure 7 shows the ET_{ref} values predicted by the data driven models and the observed values (PMFAO and PMASCE), using the data set collected by six stations from 1980 to 2010 (not used in the training and testing process).

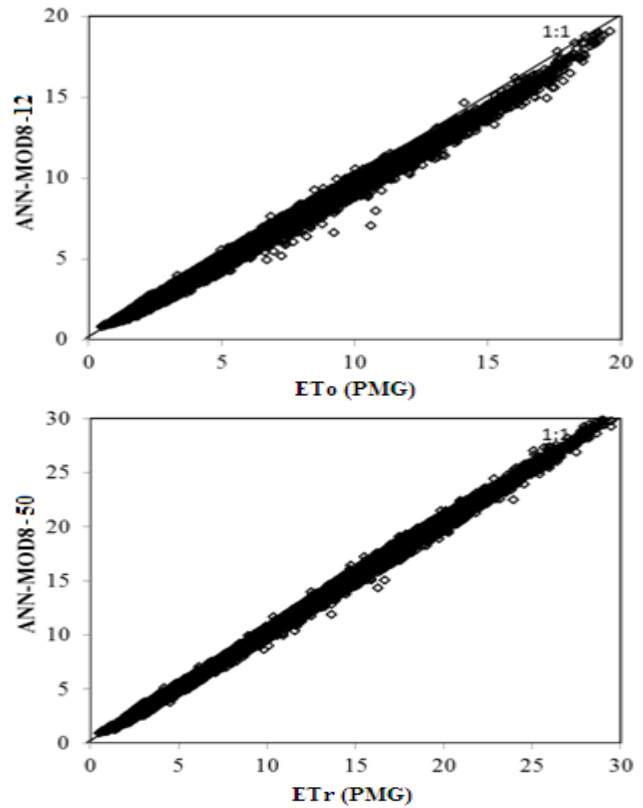


Figure 7. Comparison of the alfalfa (ET_r) and grass (ET_o) ET_{ref} estimates by ANN-MOD8-12 and ANN-MOD8-50, and the values from the PMG equation.

The figure shows that ANN-MOD8 on basis of grass (ANN-MOD8-12) had higher deviation compared to ANN-MOD8 on basis of alfalfa (ANN-MOD8-50), implying that it caused

Table 5. Statistical performance of ANN-MOD8-50 and ANN-MOD8-12 using data collected from 1980 to 2010 by six meteorological stations.

Models	R ² (%)	OI (%)	RMSE (mm/d)	MAE (mm/d)
ANN-MOD8-50	99.8	0.991	0.29	0.22
ANN-MOD8-12	99.4	0.982	0.38	0.30

greater underestimation. Table 5 shows that ANN-MOD8-50 performed better than ANN-MOD8-12 with lower error measure values and higher correlation coefficients. The R^2 and OI for ANN-MOD8-50 had also 0.4% and 0.9% more accurate than that from the ANN-MOD8-12. The ANN-MOD8-50 had a 2.4% and 2.7% decrease in the $RMSE$ and MAE under ANN-MOD8-12, receptivity.

Conclusions: Eight ANN models were developed to estimate the daily ET_{ref} under arid and hyper arid conditions. The climatic data were collected from 19 meteorological stations covering the period of 1980 to 2010. While data obtained from the 13 metrological stations were used to develop the ANN models, the data from the other six stations were used for spatial validation of the eight developed ANN models. The best performed ANN model, i.e. ANN-MOD8, was that included all climatic parameters in comparison with PM model. On the other hand, the ANN model with the temperature as the only input climatic parameter performed the least. Compared to PM model, the ANN-MOD8 with its simple algebraic equation can perfectly predict ET_{ref} for a wide range of h_c varying from 5 cm to 105 cm. An interesting result of the current study revealed that the ANN-MOD5, ANN model with no R_s , can compete with ANN-MOD8 considered the most accurate model to predict the daily ET_{ref} under the hyper arid environment. This inserting outcome leads to a possible conclusion that the climatic parameter U_2 is more important than R_s under the circumstances of this study. Furthermore, it is observed that ANN model consisting of all the input parameters with $h_c=50$ cm was found to perform better than with $h_c=12$ cm. Therefore, the ANN technique can be very helpful when applying in irrigation scheduling and management of agriculture water resources.

Acknowledgments: The project was financially supported by King Saud University, Vice Deanship of Research Chairs. Moreover, the climatic data used in this study were obtained from the Presidency of Meteorology and Environment (PME), Kingdom of Saudi Arabia. The authors highly appreciate this effort and would like thank PME for continues collaboration of providing the data.

REFERENCES

- Alazba, A.A. 2004. Estimating palm water requirements using Penman-Monteith mathematical model. *J. King Saud Univ.* 16:137-152.
- Ali, M.H. 2010. *Fundamentals of Irrigation and On-farm Water Management*, Vol. 1. Springer Science, Business Media, LLC.
- Allen, R.G., L.S. Pereira, D. Raes and M. Smith. 1998. *Crop evapotranspiration guidelines for computing crop water requirements*. FAO Irrigation and Drainage, Paper No. 56, Food and Agriculture Organization of the United Nations, Rome.
- ASCE-EWRI. 2005. *The ASCE standardized reference evapotranspiration equation*. Environmental and Water Resources, Institute of the American Society of Civil Engineers Task Committee on Standardization of Reference Evapotranspiration Calculation, Washington, DC, USA, p.70.
- Chattopadhyay, S., R. Jain and G. Chattopadhyay. 2009. Estimating potential evapotranspiration from limited weather data over Gangetic West Bengal, India: a neurocomputing approach. *Meteorol. Appl.* 16:403-411.
- Chiew, F.H.S., N.N. Kamaladassa, H.M. Malano and T.A. McMahon. 1995. Penman-Monteith, FAO-24 reference crop evapotranspiration and class-A pan data in Australia. *Agric. Water Manage.* 28:9-21.
- Dai, X., H. Shi, Y. Li, Z. Ouyang and Z. Huo. 2009. Artificial neural network models for estimating regional reference evapotranspiration based on climate factors. *Hydrol. Process.* 23:442-450.
- Dawson, W.C. and R. Wilby. 1998. An artificial neural networks approach to rainfall-runoff modeling. *Hydrol. Sci. J.* 43:47-66.
- De Souza, F. and R.E. Yoder. 1994. ET estimation in the north east of Brazil: Hargreaves or Penman-Monteith equation. *Proc. Technical Paper ASAE International Winter Meeting, American Society of Agricultural Engineers, St. Joseph, Mich.*
- Fangmeier, D.D., W.J. Elliot, S.R. Workman, R.L. Huffman and G.O. Schwab. 2006. *Soil and Water Conservation Engineering*, 5th Ed. United States: THOMSON.
- Fisher, J.B., A. Terry, A. DeBiase, Y. Qi, M. Xu and H. Allen. 2005. Evapotranspiration models compared on a Sierra Nevada forest ecosystem. *Environ. Model. Softw.* 20:783-796.
- Fooladmand, H.R. and M. Haghghat. 2007. Spatial and temporal calibration of Hargreaves equation for calculating monthly ET_o based on Penman-Monteith method. *Irrig. Drain.* 56:439-449.
- Fooladmand, H.R., H. Zandilak and M.H. Ravanani. 2008. Comparison of different types of Hargreaves equation for estimating monthly evapotranspiration in the south of Iran. *Arch. Agron. Soil Sci.* 54:321-330.

- Gavilan, P., J. Berengena and R.G. Allen. 2007. Measuring versus estimating net radiation and soil heat flux: Impact on Penman-Monteith reference ET estimates in semiarid regions. *Agric. Water Manage.* 89:275-286.
- Gavilan, P., I.J. Lorite, S. Tornero and J. Berengena. 2006. Regional calibration of Hargreaves equation for estimating reference ET in a semiarid environment. *Agric. Water Manage.* 81:257-281.
- George, B.A., B.R.S. Reddy, N.S. Raghuvanshi and W.W. Wallender. 2002. Decision support system for estimating reference evapotranspiration. *J. Irrig. Drain. Eng-ASCE* 128:1-10.
- Gocic, M. and S. Trajkovic. 2010. Software for estimating reference evapotranspiration using limited weather data. *Comput. Electron. Agric.* 71:158-162.
- Gorka, L., O.B. Amais and J.L. Jose. 2008. Comparison of artificial neural network models and empirical and semi-empirical equations for daily reference evapotranspiration estimation in the Basque Country (Northern Spain). *Agric. Water Manage.* 95:553-565.
- Haykin, S. 1999. *Neural networks. A comprehensive foundation.* Prentice Hall International Inc., New Jersey.
- Huo, Z., S. Feng, S. Kang and X. Dai. 2012. Artificial neural network models for reference evapotranspiration in an arid area of northwest China. *J. Arid Environ.* 82:81-90.
- Hupet, F. and M. Vanclooster. 2001. Effect of the sampling frequency of meteorological variables on the estimation of the reference evapotranspiration. *J. Hydrol.* 243:192-204.
- Irmak, S., A. Irmak, R.G. Allen and J.W. Jones. 2003. Solar and net radiation based equations to estimate reference evapotranspiration in humid climates. *J. Irrig. Drain. Eng.* 129:336-347.
- Izadifar, Z. 2010. Modeling and analysis of actual evapotranspiration using data driven and Wavelet techniques. Master Thesis, University of Saskatchewan, Saskatoon, Saskatchewan, Canada.
- Jain, S.K., P.C. Nayak and K.P. Sudhir. 2008. Models for estimating evapotranspiration using artificial neural networks, and their physical interpretation. *Hydrol. Process.* 22:2225-2234.
- Jensen, M.E., R.D. Burman and R.G. Allen. 1990. Evapotranspiration and irrigation water requirements. *ASCE Manuals and Reports on Engineering Practices No. 70.*, Am. Soc. Civil Engrs., New York, NY, p.360.
- Kişi, O. 2006. Generalized regression neural networks for evapotranspiration modeling. *Hydrol. Sci. J.* 51:1092-1105.
- Kişi, O. 2007. Evapotranspiration modeling from climatic data using aneural computing technique. *Hydrol. Process.* 21:1925-1934.
- Kişi, O. and O. Oztürk. 2007. Adaptive neuro-fuzzy computing technique for evapotranspiration estimation. *J. Irrig. Drain. Engr.* 133:68-379.
- Kumar, M., A. Bandyopadhyay, N.S. Raghuvanshi and R. Singh. 2008. Comparative study of conventional and artificial neural network based reference evapotranspiration estimation models. *Irrig. Sci.* 26:531-545.
- Kumar, M., N.S. Raghuvanshi and R. Singh. 2011. Artificial neural networks approach in evapotranspiration modeling: a review. *Irrig. Sci.* 29:11-25.
- Kumar, M., N.S. Raghuvanshi, R. Singh, W.W. Wallender and W.O. Pruitt. 2002. Estimating evapotranspiration using artificial neural network. *J. Irrig. Drain. Engr.* 128:224-233.
- Landeras, G., A.O. Barredo and J.J. Lopez. 2008. Comparison of artificial neural network models and empirical and semi-empirical equations for daily reference evapotranspiration estimation in the Basque Country (Northern Spain). *Agric. Water Manage.* 95:553-565.
- Li, F.Z. and A. Beswick. 2005. Sensitivity of the FAO-56 crop reference evapotranspiration to different input data. Technical report. Queensland Government, Natural Resources and Mines; pp.1-14.
- Monteith, J.L. 1965. The state and movement of water in living organisms. In *Proceedings, Evaporation and Environment, XIXth Symp.*, Soc. For Exp. Biol., Swansea. Cambridge Univ. Press: New York, pp.205-234.
- Monteith, J.L. 1973. *Principles of Environmental Physics.* Edward Arnold: London.
- Naoum, S. and K.I. Tsanis. 2003. Hydroinformatics in evapotranspiration estimation. *Environ. Model. Softw.* 18:261-271.
- Sabziparvar, A.A. and H. Tabari. 2010. Regional estimation of reference evapotranspiration in arid and semiarid regions. *J. Irrig. Drain. Eng-ASCE* 136:724-731.
- Saudi Geological Survey. 2012. *King Saudi Arabia: Facts and Numbers*, Ed 1.
- Smith, M., R.G. Allen, J.L. Monteith, L.S. Pereira, A. Perrier and W.O. Pruitt. 1991. Report on the Expert Consultation on Revision of FAO Guidelines for Crop Water Requirements, Land and Water Development Division, FAO, Rome.
- Sudheer, K.P., A.K. Gosain and K.S. Ramasastri. 2003. Estimating actual evapotranspiration from limited climatic data using neural computing technique. *J. Irrig. Drain. Eng-ASCE.* 129:214-218.
- Tabari, H. 2010. Evaluation of reference crop evapotranspiration equations in various climates. *Water Resour. Manage.* 24:2311-2337.
- Tabari, H. and P. Talae. 2011. Local calibration of the Hargreaves and Priestley-Taylor equations for estimating reference evapotranspiration in arid and cold climates of Iran based on the Penman-Monteith model. *J. Hydrol. Eng.* 16:837-845.
- Temesgen, B., S. Eching, B. Davidoff and K. Frame. 2005.

- Comparison of some reference evapotranspiration equations for California. *J. Irrig. Drain. Eng-ASCE* 131:73-84.
- Trajkovic, S. 2005. Temperature-based approaches for estimating reference evapotranspiration. *J. Irrig. Drain. Eng-ASCE* 131:316-323.
- Traore, S., Y-M. Wang and T. Kerh. 2010. Artificial neural network for modeling reference evapotranspiration complex process in Sudano-Sahelian zone. *Agric. Water Manage.* 97:707-714.
- Walter, I.A., R.G. Allen, R. Elliott, D. Itenfisu, P. Brown, M.E. Jensen, B. Mecham, T.A. Howell, R. Snyder, S. Echings, T. Spofford, M. Hattendorf, D. Martin, R.H. Cuenca and J.L. Wright. 2001. The ASCE standardized reference evapotranspiration equation. Environmental and Water Resources Institute (EWRI) of the ASCE.
- Xiaoying, L., L. Erda. 2005. Performance of the Priestley-Taylor equation in the semi-arid climate of North China. *Agric. Water Manage.* 71:1-17.
- Xu, C.Y. and V.P. Singh. 2001. Evaluation and generalization of temperature based equations for calculating evaporation. *Hydrol. Process.* 15:305-319.
- Xu, C.Y. and V.P. Singh. 2002. Cross comparison of empirical equations for calculating potential evapotranspiration with data from Switzerland. *Water Resour. Manag.* 16:197-219.
- Yin, Y., S. Wu, D. Zheng and Q. Yang. 2008. Radiation calibration of FAO56 Penman-Monteith model to estimate reference crop evapotranspiration in China. *Agric. Water Manage.* 95:77-84.
- Zanetti, S.S., E.F. Sousa, V.P.S. Oliveira, F.T. Almeida and S. Bernardo. 2007. Estimating evapotranspiration using artificial neural network and minimum climatological data. *J. Irrig. Drain. Eng-ASCE* 133:83-89.